Strain-Induced Martensite Formation and its Influence on the Damage Behaviour under Monotonic and Cyclic Loading

Carsten Müller-Bollenhagen[1,a], Martina Zimmermann[1,b], Hans-Jürgen Christ[1,c]

[1]Institut für Werkstofftechnik, Universität Siegen, Paul-Bonatz-Str. 9-11, 57068 Siegen, Germany

[a]carsten.mueller-bollenhagen@uni-siegen.de, [b]martina.zimmermann@uni-siegen.de, [c]hans-juergen.christ@uni-siegen.de

Keywords: deformation-induced martensite, austenitic stainless steel sheet, very high cycle fatigue (VHCF)

Abstract

Metastable austenitic stainless steels are known to undergo a partial transformation of austenite into martensite as a consequence of plastic deformation. This transformation process depends on the chemical composition (and in particular the carbon concentration), the strain amplitude as well as the strain rate, the temperature and the grain size. Those influence factors are systematically analysed in order to establish a reliable data basis for a quantitative prediction of the strain-induced martensite formation and as a consequence the related damage behaviour under monotonic and cyclic loading. The material models being used to predict the strain-induced martensite formation in the study presented showed a very reasonable correlation between experimental data and simulation results. As most manufacturing processes of metallic components lead to plastic deformation in the material, the utilization of this transformation effect to adjust the monotonic and cyclic strength behaviour for the highly stressed areas of a component is evident. Prior investigations revealed a clear correlation between the fatigue life in the LCF range and the level of martensitic transformation which still has to be confirmed for the very high cycle fatigue range.

Introduction

Metastable austenitic stainless steels can undergo a deformation induced phase transformation from austenite (fcc) into ε-martensite (hcp) and α'-martensite (tetragonally distorted). Transformed α'-martensite can be used to modify monotonic [1] and cyclic [2] properties of austenitic stainless steel. This is of particular interest as austenitic stainless steels are often used for components with increasing safety requirements, like pipelines in nuclear reactors or heavy-duty automotive structures. The major aim of this study is to establish a basis for the optimization of fatigue strength of an automotive structural part - the cross tube of a trailer coupling - by setting up a specific amount of martensite during its tube-forming process. A more detailed description of this structural element and the forming process is given elsewhere [3].

The study presented aims at a comprehensive understanding of the correlation between the very high cycle fatigue (VHCF) behaviour and the martensite formation of metastable austenitic steels. Over the last decade it was shown for a number of metals that failure occurs even beyond the classical fatigue limit of $2x10^6$-10^7 cycles [4, 5]. Crack initiation gains importance at larger fatigue lives and various reports in the literature propose that localized cyclic plastic deformation and a resulting crack initiation are the dominant life controlling mechanism [e.g. 6]. Depending on the material studied, the localized plastic deformation can lead to surface as well as subsurface crack initiation, mostly occurring at persistent slip bands or at pores or inclusions, respectively. In this context so-called dual or multistage fatigue life diagrams are being discussed. In order to distinguish between the different damage mechanisms, Mughrabi [7] suggested the classification of metals in type I materials showing surface crack initiation, typically single phase ductile metals, and type II materials with inner defects such as inclusions, pores etc. showing subsurface crack initiation.

The VHCF behaviour of AISI304 has hardly been investigated yet, especially the correlation of martensite formation and very high cycle fatigue is still basically unknown. Takahashi et al. [8] studied fatigue behaviour of non-martensitic monotonically pre-deformed AISI304 specimens and observed a singular appearance of internal crack initiation ('fish eye fracture') in the VHCF regime. No defect in the crack-origin could be found. Hence the role of hard inclusions quite likely present in austenitic stainless steels in the crack initiation process at very high load cycles is not clear. Chai [9] observed subsurface non-defect fatigue crack origins in experiments with a non-predeformed martensite-austenite steel at cycles higher than 10^6 and concluded that the damage process in the VHCF range of two phase alloys can be determined by deformation mismatches in the two phases, as a consequence of their differing mechanical properties. For high cycle fatigue, Myeon et al. [10] detected a 60-fold enhancement of durability as a result of thermally induced micro-martensite particles which prevent crack initiation. Maier et al. [2] proved that there is an optimum fraction of deformation-induced martensite in ASI304 of 30-40% for the low cycle fatigue regime.

The purpose of this paper is to investigate the martensite formation under monotonic and cyclic loading and the influence of martensite formation through pre-deformation on the VHCF behaviour.

Material and Experimental Procedure

Three batches of stainless steel sheets (AISI304) were tested under monotonic tensile loading in the as-received condition. The composition, mechanical properties and calculated M_{d30}-temperatures [11] are shown in Table 1 and 2. The mean grain size varied between 21 and 25 µm for all batches. Isolated carbide inclusions with high Ti, Cr and Mn contents (acc. to EDS-analysis) and a size of 5-10 µm were found in SEM investigations.

Table 1. Chemical composition [mass-%] of the alloys studied.

	C	Cu	Cr	Mo	Ni	Mn	N
HR	0.024	0.14	18.3	0.04	8.11	1.43	0.067
WS	0.04	0.23	18.2	0.20	8.05	1.19	0.049
TK	0.03	0.4	18.2	0.22	8.15	1.29	0.068

Table 2. Tensile test data and M_{d30}-temperatures.

	Young's-Modulus [GPa]	$R_{p0,2}$ [MPa]	$R_{p0,1}$ [MPa]	R_m [MPa]	M_{d30} [°C]
HR	189.7	284	266	649	2.8
WS	190.1	286	259	687	10.4
TK	194.4	300	266	641	2.5

The volume fraction of martensite was measured by means of the magneto-inductive device *feritscope MP30* (FISCHER). All values for martensite fraction in the following are the values measured by feritsope; where applicable the value were corrected by functions taking into account variation in measured values for geometrical or loading reasons (Villari-Effect). The aspect that results measured via feritscope might underestimate the true martensite fraction [12] will be further investigated.

For the tensile tests at room temperature an electromechanical testing machine (ZWICK) was used. For the tensile tests below room temperature a hydraulic testing machine (SCHENK) equipped with a liquid-nitrogen-cooled chamber was used. All tensile tests were performed with in-situ measurements of temperature and martensite content (feritscope).

For the fatigue experiments a resonance pulsating high frequency test system (RUMUL) operating at 90 Hz (with sheet specimens) and an ultrasonic testing machine operating with a test frequency of 20 kHz was used. The vibrating parts of the ultrasonic testing system are designed in a way that under resonance conditions a standing wave develops along the major load axis with a maximum stress/strain amplitude in the center region of the specimen (Fig. 1). At this center region strain gauges are used to measure the strain amplitude. A cyclic stress-strain curve, registered during the resonance pulsating experiments, was used to determine the corresponding stress amplitude for any such measured strain amplitude. The fatigue tests were conducted under axial tension-compression loading with a stress ratio R = -1 in ambient air, applying intermitting pulse and pause sequences for the ultrasonic testing (pulse/pause length: 90 ms/2000 ms).

Temperature was measured at three points of the specimen with a thermal infrared camera (FLIR A20-M) and K-type thermocouples. As has been proposed by Smaga et al. [13] the change of temperature ΔT was used to describe the cyclic deformation behaviour. The location of the measured temperatures and the specimen geometry used are illustrated in Fig. 2. ΔT was calculated using the equation

$$\Delta T = T_1 - 0.5\,(T_2 + T_3). \tag{1}$$

According to [14, 15] load-increase tests accompanied by high-resolution temperature measurement can be used to estimate the fatigue limit of metals. This method was used at the resonance pulsating test system for a preliminary comparison of the fatigue limits of specimens with different martensite fractions.

Fatigue experiments executed by means of the resonant vibrating system were stopped after 10^8 cycles, ultrasonic fatigue tests after 10^9 cycles, specimens without crack initiation thus being denoted as run-outs. Specimens were electrolytically polished. Because of its low thermal conductivity, good damping properties and relatively high plastic deformation, the used material showed a strong development of heat and the testing at both systems required an active cooling with compressed air.

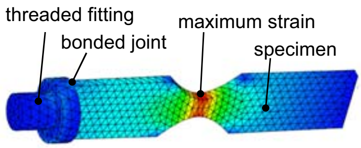

Fig. 1. Stress distribution and specimen design for the ultrasonic testing (thickness: 2mm)

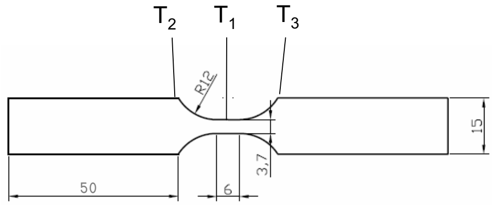

Fig. 2. Specimen design and points of temperature measurement for the resonance pulsating test system (thickness: 2mm)

Results

Martensite formation and damage behaviour under monotonic loading. Tensile tests were performed to quantify the major factors affecting deformation-induced martensite formation. Different start temperatures during tensile testing can be used to adjust the quasi-static mechanical properties, Fig. 3. With a decrease of the specimens initial temperature from 23°C to -20°C the stress-strain curve changes from a parabolic to a more sigmoidal shape caused by an increasing volume of α’-martensite. This leads to an increase in tensile strength of about 42 % and a decrease in elongation at fracture.

Furthermore, it can be stated that the martensite formation strongly depends on the batch-specific chemical composition. Fig. 4 correlates reasonably with the M_{d30} temperatures in Table 2, with the batch HR having the strongest affinity to martensite formation and batch TK the weakest. However, M_{d30} can only give a coarse account of the austenite stability, as the significant differences in martensite formation of batches HR and WS in Fig. 4 was not expected. Moreover, the strain rate strongly influenced the martensite formation during tensile testing.

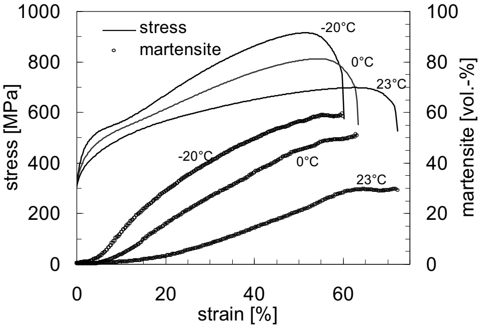

Fig. 3. Martensite formation in tensile tests with different start temperatures (batch HR)

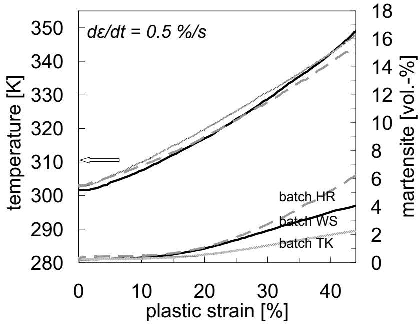

Fig. 4. Influence of batch variation on martensite formation

The tensile test results were used to determine the consistency of acknowledged material models from literature to predict the martensite formation resulting from a monotonic uniaxial deformation. Three models proposed by Springub et al. [16], Heinemann [17] and Picozzi et al. [18] were surveyed. Because of the mentioned batch variations it is necessary to fit specific constants for each model with batch-specific tensile test data. All models show a satisfactory agreement between experimental and calculated data for tensile tests at room temperature for the batch HR. Further investigations with varying parameters (strain rate, ambient temperature etc.) will lead to a precise evaluation of the existing models' ability to predict martensite formation in sheet forming processes.

Damage behaviour under cyclic loading. Fatigue tests were conducted in order to characterize the VHCF behaviour of AISI304 in fully austenitic and partially martensitic state. Only specimens made of batch HR were fatigued, because this batch showed the strongest affinity to martensite formation. A distinct cyclic softening followed by a cyclic hardening could be observed during all fatigue experiments, even though stress amplitudes were considerably below $R_{p0.2}$ and even below the fatigue limit at 10^8 cycles. Fig. 5 shows an increase in ΔT up to about $7x10^4$ cycles followed by cyclic softening (indicated by a decrease in ΔT) up to approx. 3 x 10^6 cycles for a run-out specimen at σ_a = 240MPa. The same trend exists for the course of the test frequency, that is the resonance frequency of the specimen-machine system (Fig. 5). Both parameters, temperature and test frequency, can be used to survey the transient behaviour of the material during cyclic deformation. Frequency changes attributed to machine parameters or other external influence factors can be excluded, as testing conditions were kept constant. The correlation of plastic strain and ΔT was proven by recording the stress-strain hysteresis loop. The temperature and frequency changes during the initial 10^6 cycles illustrate that the material studied does experience global plastic deformation before reaching a saturation stage. For this reason, the damage mechanism in the VHCF region cannot be reduced to the phenomenon of imhomogeneously distributed local plastic deformation. The global plastic deformation, as is shown in Fig. 5, has to be considered, too.

Load-increase tests were performed to estimate the fatigue limit of the material studied on the basis of ΔT. In Fig. 6 the changes in temperature ΔT for two fully austenitic, non-predeformed specimens during a stepwise load increase test are plotted versus the number of cycles. During the test sequence the stress amplitude was increased by 10 MPa each 10^4 cycles. In order to avoid any unwanted influences due to slightly different cooling conditions no active cooling was applied during the load increase tests. In Fig. 6 it can be seen that the change of temperature ΔT rises with every step but converges to a horizontal asymptote within every step up to 240 MPa, where it starts to rise significantly. Assuming that this load step indicates the stress amplitude where considerable plastic deformation starts, 240MPa can be taken as first estimation of the fatigue limit.

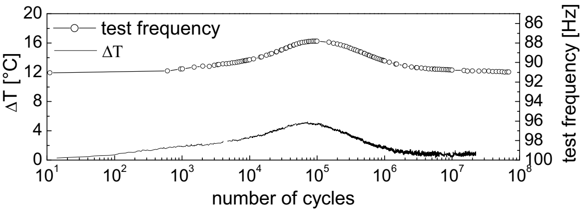

Fig. 5. ΔT and test frequency during cyclic deformation of a run-out specimen (σ_a=240MPa)

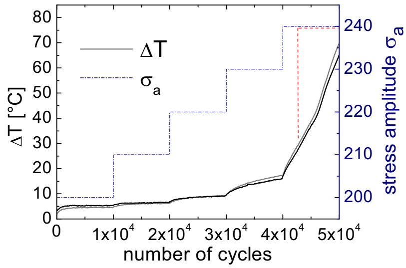

Fig. 6. Load-increase tests with fully austenitic specimen

This assessment of fatigue limit was subsequently confirmed by means of constant amplitude tests. The results are shown in Fig. 7. Tests were executed on the resonance pulsating system up to 10^8 cycles. The fatigue limit resulting from constant amplitude tests is 250 MPa. No failure occurred between 10^6 and 10^8 cycles. All failed specimens were loaded above a stress amplitude of 250 MPa. Metallographic analysis of the fracture surfaces proved that no subsurface crack initiation occurred.

As the investigated material shows considerable cyclic hardening and softening, the ultrasonic system could not be used to cycle specimens up to 10^6 cycles. The closed loop control system of the ultrasonic system is only reliable, when the global plastic deformation is small. For that reason specimens where cycled up to 10^6 by means of the resonance pulsating system, thus reaching the cyclic saturation stage (Fig. 5). Afterwards specimens were fatigued by ultrasonic testing up to 10^9 cycles. The load amplitude for the ultrasonic system was calibrated based on a cyclic stress-strain curve recorded for several specimens at 10^6 cycles with the resonance pulsating system by the use of strain gauges. The results of two ultrasonic fatigued specimens are shown in Fig. 7, both are run-outs and support the fatigue limit at 250 MPa. Slip bands and α'-martensite needles in isolated grains at the surface of all run-out specimens are an indication of local plastic deformation, e. g. α'-martensite needles after 10^9 cycles can be seen in Fig. 8.

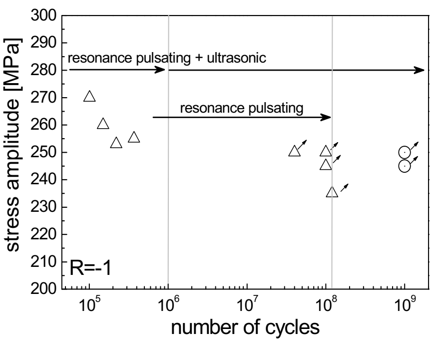

Fig. 7. S-N curve of specimens fatigued by resonance pulsation and ultrasonic testing system (arrows indicate run-out specimens).

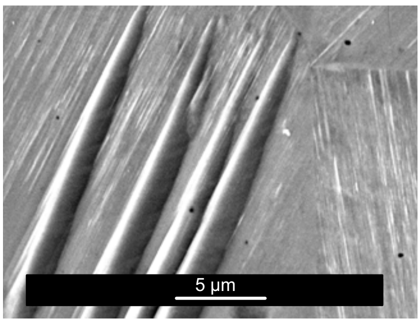

Fig. 8. Formation of martensite after 10^9 cycles, 245 MPa.

Load-increase tests were used to study the dependence of the fatigue limit of austenitic specimens on the deformation-induced martensite content. The different martensite contents were adjusted by means of a 15% elongation by a tensile load at different temperatures below room temperature. Subsequently these specimens were fatigued by load-increase tests with a step length of 10^4 cycles and a step height of 5 MPa. In Fig. 9, the results for four specimens containing volume fractions from 1% up to 34% martensite are shown. All tests ended with the failure of the specimen. Comparing the samples with 1% and 19% martensite fraction, a strong increase in the stress amplitude which leads to a significant temperature change indicating specimen failure can be observed (from 345 MPa to 380 MPa). However, with increasing martensite content (26% and 32%) the stress amplitude resulting in specimen failure and abrupt rise in ΔT decreases again (green and black lines in Fig. 9). Hence a first trend towards an optimal martensite volume below 26% with regard to fatigue limit can be assumed. Constant amplitude tests with varying martensite contents will be executed to verify the estimated optimal martensite content during the continuation of the ongoing work.

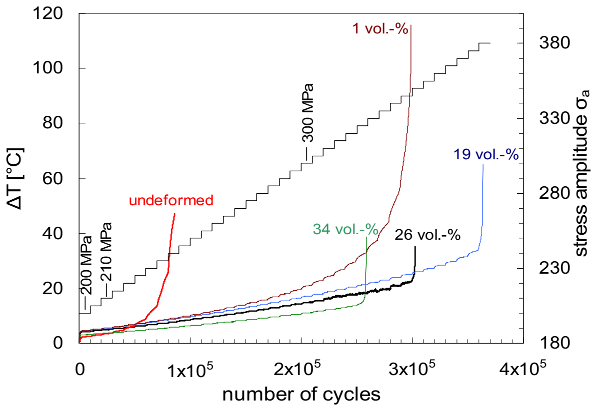

Fig. 9. Load-increase tests with specimens of different martensite content.

Summary

The influence of deformation induced martensite formation on the monotonic and cyclic strength of a metastable austenitic steel was studied with the following results:

- The susceptibility of the austenitic phase to deformation-induced martensite formation is strongly affected by temperature, strain rate and slight variations in the chemical composition.
- Constitutive material models to predict the martensite volume fraction show a satisfactory accordance between test and calculated data for tensile tests at room temperature.
- The fatigue limit was estimated on the basis of load-increase tests with a difference of 10 MPa in comparison with the fatigue limit derived from constant amplitude tests.
- The cyclic deformation was dominated by pronounced cyclic hardening and softening up to a number of cycles of 10^6 merging into a saturation stage for the remaining fatigue test.
- No specimens in the undeformed condition failed in the very high cycle fatigue range, even though slip markings could be observed in most grains and martensite formation in some grains on the samples's surface.

- The fatigue behaviour on the basis of load increase tests of the predeformed specimens showed an optimum for a martensite volume fraction below 26%.

Acknowledgement

The authors gratefully acknowledge financial support of this study by Deutsche Forschungsgemeinschaft.

References

[1] S. S. Hecker, M. G. Stout, K. P. Staudhammer, J. L Smith: Metall. Trans. A, Vol. 13A (1982), p. 619-626.

[2] H. J. Maier, B. Donth, M. Bayerlein, H. Mughrabi, B. Maier, M. Kesten: Z. Metallkd., Vol. 84 (1993), No. 12, p. 820-26.

[3] C. Müller-Bollenhagen, M. Zimmermann, H-J. Christ, X. Schröder, B. Engel, A. Große-Wöhrmann, F.-T. Suttmeier: submitted to Steel Res. Int. (2008).

[4] Y. Murakami, T.Nomoto, T. Ueda: Fatigue & Fract. Engng. Mater. Struct., Vol. 22 (1999), p. 581-590.

[5] M. Papakyriacou, H. Mayer, C. Pypen, H. Plenk, Jr., S. Stanzl-Tschegg: Mater. Sci. Eng. A, Vol. 308 (2001), No. 1-2, p. 143-152.

[6] P. Lukáŝ, L. Kunz: Fatigue & Fract. Engng. Mater. Struct., Vol. 25 (2002), No. 8-9, p. 747-753.

[7] H. Mughrabi: Fatigue & Fract. Engng. Mater. Struct., Vol. 25 (2002), No. 8-9, p. 755-764.

[8] K. Takahashi, T. Ogawa: Trans. Jpn. Soc. Mech. Eng. A, Vol. 72 (2006), p. 1731/36.

[9] G. Chai: Proc. of 3. Int. Conf. on Very High Cycle Fatigue (VHCF-3), Japan (2004), p. 24-31.

[10] T. H. Myeon, Y. Yamabayashi: M. Shimojo, Y. Higo: Int. J. Fatigue, Vol. 19 (1997), No. 93, p. 69-73.

[11] K. Nohara, Y. Ono, N. Ohashi: J. Iron Steel Inst. Jpn, Vol. 63 (1977), No. 5, p. 212-22.

[12] J. Talonen, P. Aspergren, H. Hänninen: Mat. Sci. Tech., Vol. 20 (2004), p. 1506-1512.

[13] M. Smaga, F. Walther, D. Eifler: Int. J. Mat. Res., Vol. 97 (2006), No. 12, p. 1648-55.

[14] V. Wagner, B. Ebel-Wolf, F. Walther, D. Eifler: J. E. Allison, J. W. Jones, J. M. Larsen, R. O. Ritchie (Ed.), Proc. of the 4. Int. Conf. on Very High Cycle Fatigue, TMS Publications (2007), 137-142.

[15] D. Dengel, H. Harig: Fatigue Fract Eng M, Vol. 3 (1980), p. 113-128.

[16] B. Springub, B. A. Behrens, E. Doege: Steel Res. Int., Vol. 75 (2004), No. 7, p. 475-482.

[17] G. Heinemann: Virtuelle Bestimmung des Verfestigungsverhaltens von Bändern und Blechen durch verformungsinduzierte Martensitbildung bei metastabilen rostfreien austenitischen Stählen, Doctorate Thesis, ETH Zürich (2004).

[18] V. Piccozi, R. Sanchez, P. Bolt: Final Report on the project EUR 21143, Technical Steel Research, European Commission, Luxemburg (2004), ISBN 92-894-8097-1.